

Model of the Compressing Process of a One- and Two-Side Fastened Connector of a 3D Distance Knitted Fabric

Abstract

A model of the compressing process of a 3D distance knitted fabric was related to a single connector fastened on one side by an articulated joint, as well as fastened on both sides by fixed joints, considering the connector as a slender rod with an assumed shape. The compressing of an elastic rod in the physical and mathematical models was based on assumptions considering the morphology of the knitted fabric as well as the mechanical properties of threads – monofilaments placed in the internal layer of the knitted fabric. Calculation methods and algorithms were developed for the determination of the functional dependencies between the force compressing the knitted fabric and deflection, as well as the description of the curves representing the shape of the compressed rod. A computer simulation of compressing the rod, which connects both outside layers of the knitted fabric, was carried out with the use of the 'Mathematica' program, taking into consideration the variable parameters of the model. The considerations carried out in this article are significantly based on our previous publication, and therefore the assumptions of the physical model and detailed descriptions of the analysis are not included.

Key words: knitted 3D fabrics, distance fabrics, compression process, connector, articulated joint, mathematical model, physical model.

Introduction

The work presented herein is a continuation and broadening of the theoretical considerations of compressing a single connector joining the two outside planes of a distance knitted fabric carried out in our previous work. The models described below selectively concern the following different fastening variants: two-side articulated joints and one-side and two-side fixed joints. Considering the particular cases, we assumed that no mutual displacement of the outside planes take place. However, praxis indicated that, in the case of some stitches of the knitted distance fabric, the outside planes displace mutually during compression.

The fastening variants of the connector we assumed were not randomly chosen. The model of articulated fastenings is related to empirically stated shapes of a compressed monofilament in the 3D system.

The model presented in this paper considering the two-side fastening of the connector by fixed joints is related to a knitted fabric with a compact structure of the outside layers, which are sometimes even laminated. On the other hand, the system with a one-side articulated joint of the connector may be related to a loose knitted fabric with a small cover factor of one of the knitted fabric's outside layers.

Physical model of the compressing process

Below are presented physical models of compressing a slender, elastic rod with an assumed shape. The general assumption accepted the fastening of the rods as one side articulated and both sides fixed [2-7].

Figure 1 presents a physical model with the following designations: g_0 – initial fabric thickness, g_i – fabric thickness during deflection, Δg – deflection (deformation) of the rod, p_1, p_2 – planes including the knitted fabric's loops, y_0 – difference in the positions of the rod in the longitudinal direction (y), P_1 – force compressing the bent rod, S_1 – transversal force of the reaction of the base.

Mathematical models of the compressing process of a single connector

The above-presented physical models allow us to formulate differential equations of the fourth order that connect the loading of the rod with its deformations. We consider the rod (connector) discussed as two separate rods formed by its projection on the planes Oxz and Oyz .

The differential equation that describes the deformations of the rod influenced by the loads has the following form:

$$EJy''(x) = -P_1y'(x) + S_1x \quad (1)$$

where: $y(x) = y_0(x) + y_1(x)$

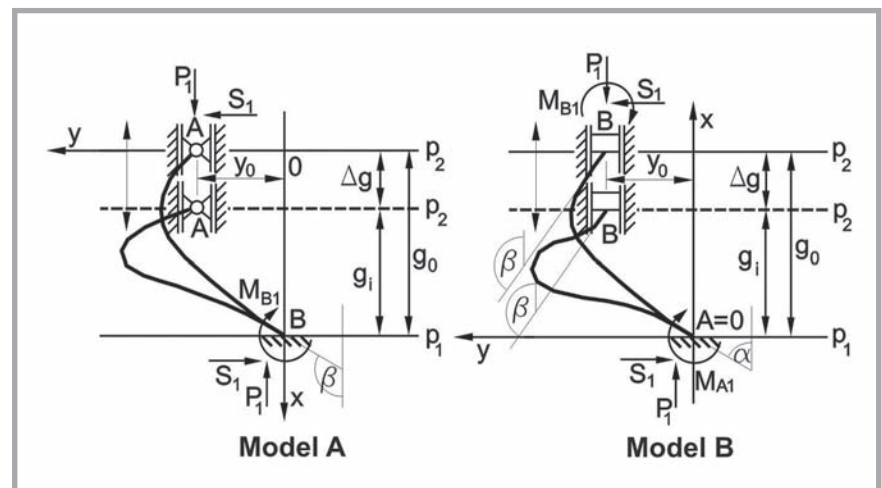


Figure 1. Scheme of physical models of the compressed and bent elastic rod; A – model of a one-side fixed rod, B – model of a both-sides fixed rod.

where:

$y_0(x)$ and $y_1(x)$ are the initial buckling, and the buckling occurring as a result of the force P_1 action, respectively;

S_1 – is the force of reaction of the transversal, sliding support,

E – is the Young modulus, and

J – is the modulus of inertia of the bent object's cross section.

Differentiating twice the Equation (1) toward 'x', we obtain subsequently:

$$y''''(x) = \frac{P_1 y'(x) - S_1}{EJ} \quad \text{and} \quad y''''(x) = \frac{P_1 y''(x)}{EJ}$$

where: $y(x) = y_0(x) + y_1(x)$. (1.a)

Equation (1.a) finally takes the form:

$$y''''(x) + k_1^2 y''(x) = 0$$

where: $k_1^2 = \frac{P_1}{EJ}$.

The general integral of Equation (1) may be written in the form of (Equation 2).

We determine the integration constants C_{11} , C_{21} , C_{31} , and C_{41} for model A in **Figure 1** from the following boundary conditions (Equation 3).

On the other hand, we determine the integration constants C_{11} , C_{21} , C_{31} , and C_{41} for model B in **Figure 1** from the following set of boundary conditions (Equation 4).

The descriptions of the integration constants C_{11} , C_{21} , C_{31} , and C_{41} obtained from the equation system are not presented in this paper, taking into consideration their very complex shape.

For model A, we find the dependency connecting force P_1 with deformation Δg in the form of an implicit function $f(P_1, \Delta g) = I_p$ by substituting the integration constants C_{11} , C_{21} , C_{31} , and C_{41} determined from the equation system (3) into the condition of the length of the bent rod, and finally obtain (Equation 5).

Similarly as for model A, for model B we find the dependency connecting force P_1 with deformation Δg in the form of an implicit function $f(P_1, \Delta g) = I_p$ by substituting the integration constants C_{11} , C_{21} , C_{31} , and C_{41} determined from the equation system (4) into the condition of the length of the bent rod, and finally obtain (Equation 6).

Figure 2 presents the mechanical characteristics of the compressed monofilament for the variants A and B [9], as well as the variant described in the previous article [8] – the rod connected by two artificial joints.

The curves have a strongly non-linear character (a great increase in the bending force P_1 at the greatest deflections of the rod). The mechanical characteristics $P_1 = f(\Delta g)$ have a similar character to the characteristics obtained empirically [8]. Notwithstanding that the mathematical analysis carried out concerns a single monofilament, thanks to the assumption that we have made concerning the physical model, it is possible to obtain a generalised characteristic for the whole knitted fabric with the additional assumption that all connectors have the same geometrical form. In order to do this, only the force compressing the whole fabric should be divided by

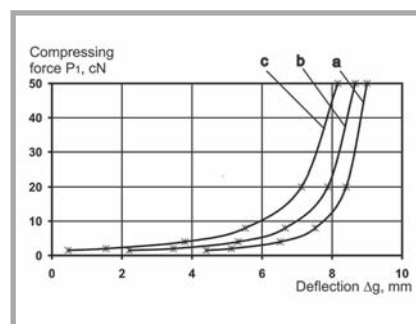


Figure 2. Mechanical characteristics $P_1 = f(\Delta g)$ of a compressed monofilament for three variants: a) two articulated fastenings, b) one articulated and one fixed fastening, c) two fixed fastenings.

the number of connectors, and for the force obtained, the mechanical characteristic $P_1 = f(\Delta g)$ should be designed.

The data of comparable results obtained by the mathematical simulation and by experimental tests obtained with the use of a specially designed measuring stand are not included in this article as the stand is actually undergoing further investigation, but they will be the subject of a subsequent publication.

The rod described by model B is the least susceptible to load, whereas the model described in the previous article is the most susceptible. For example, for model B a force $P_1 = 20$ cN causes deformation $\Delta g = 7.2$ mm, whereas for model A the deformation will be $\Delta g = 7.8$ mm, and for the model with articulated joints at both sides, $\Delta g = 8.2$ mm.

The mechanical characteristics determined are the basis for further more

$$y(x) = C_{11} + C_{21}x + C_{31} \sin(k_1 x) + C_{41} \cos(k_1 x) \quad (2)$$

$$y(\Delta g) = y_0 \rightarrow C_{11} + C_{21}\Delta g + C_{31} \sin(k_1 \Delta g) + C_{41} \cos(k_1 \Delta g) = y_0, \quad y(g_0) = 0 \rightarrow C_{11} + C_{21}g_0 + C_{31} \sin(k_1 g_0) + C_{41} \cos(k_1 g_0) = 0 \quad (3)$$

$$y'(g_0) = tg\beta \rightarrow C_{21} + C_{31}k_1 \cos(k_1 g_0) - C_{41}k_1 \sin(k_1 g_0) = tg\beta, \quad y''(\Delta g) = 0 \rightarrow -C_{31}k_1^2 \cos(k_1 \Delta g) - C_{41}k_1^2 \sin(k_1 \Delta g) = 0$$

$$y(0) = 0 \rightarrow C_{11} + C_{41} = 0, \quad y(g_i) = y_0 \rightarrow C_{11} + C_{21}g_i + C_{31} \sin(k_1 g_i) + C_{41} \cos(k_1 g_i) = y_0 \quad (4)$$

$$y'(0) = tg\alpha \rightarrow C_{21} + C_{31}k_1 = tg\alpha, \quad y'(g_i) = tg\beta \rightarrow C_{21} + C_{31}k_1 \cos(k_1 g_i) - C_{41}k_1 \sin(k_1 g_i) = tg\beta$$

$$\sum_{j=1}^n \sqrt{\{C_{21} \frac{g_i}{n} + C_{31}[\sin(k_1(\Delta g + j \frac{g_i}{n})) - \sin(k_1(\Delta g + (j-1) \frac{g_i}{n}))] + C_{41}[\cos(k_1(\Delta g + j \frac{g_i}{n})) - \cos(k_1(\Delta g + (j-1) \frac{g_i}{n}))]\}^2 + (\frac{g_i}{n})^2} = I_p \quad (5)$$

$$\sum_{j=1}^n \sqrt{\{C_{21} \frac{g_i}{n} + C_{31}[\sin(k_1 j \frac{g_i}{n}) - \sin(k_1(j-1) \frac{g_i}{n})] + C_{41}[\cos(k_1 j \frac{g_i}{n}) - \cos(k_1(j-1) \frac{g_i}{n})]\}^2 + (\frac{g_i}{n})^2} = I_p \quad (6)$$

Equations 2, 3, 4, 5 and 6.

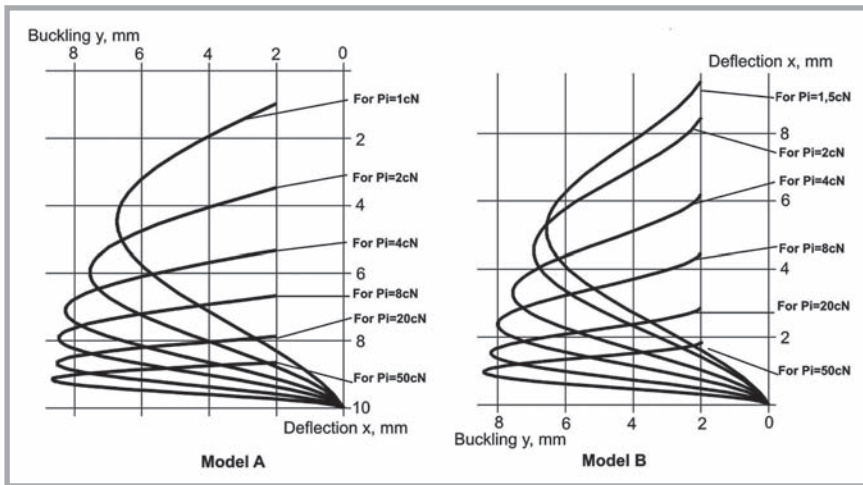


Figure 3. Simulated deflection lines of the rod formed as the effect of the force P_1 impact.

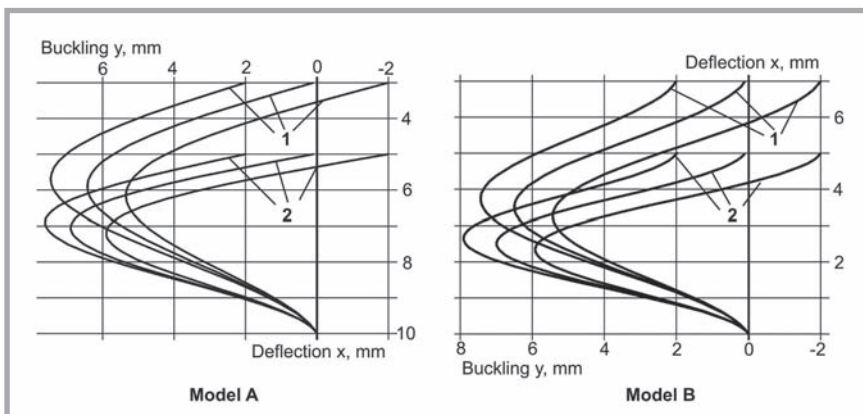


Figure 4. Family of curves representing the shape of the monofilament with the same deformations Δg and differentiated by parameter y_0 .

complex considerations concerned with the structure and strength properties of 3D distance knitted fabrics. The hitherto discussed calculation model takes into consideration only a simple loading system that uniformly loads all the monofilaments of the compressed knitted fabric. While using more complex loading systems, such as convex plates or ball-like ended pistons, the compressed outside layer of the 3D knitted fabric deforms. However, this does not change the fact that the sum of action of the individual connectors contributes to the total effect of compressing the fabric. The connectors are deformed differentially, and take different loads according to the mechanical characteristic $P_1 = f(\Delta g)$.

Simulation of the compressing process on the basis of mathematical models

The first simulation presented shows the shapes of the monofilament under the action of force P_1 . Observation of the con-

nectors' geometry, as well as the mathematical analysis, [9] shows that the rod representing the monofilament takes the shape of a fragment of a sinusoid. The shape of this curve depends on the value of the force P_1 . With an increase in the force value, an increase in the amplitude of the curve occurs, but the curve tends to be narrower. The cause of increasing P_1 is, from the physical point of view, a decrease in the curvature radius of the sinusoid apex. Figure 3 presents a broad spectrum of deflections caused by force P_1 .

The compressing curves of both variants considered do not differ much apart on the difference that in the model B a curvature of the upper part of the rod occurred, caused by the fastening. This curvature, causing the rod to compress according to model B, is less susceptible to deformation than the rod of model A.

The second simulation was aimed to check the influence of the geometry of the distance knitted fabric on the value

of compressing force P_1 . Essential here is the influence of the difference in the fastening positions of the rod in the longitudinal direction (parameter y_0 in Figure 1) on the value of this force. The parameter y_0 takes two different values: if the system is symmetric, then $y_0 \approx 0$ mm; if it is asymmetric, then $y_0 = \pm 2$ mm.

Figure 4 presents two families of curves that represent the shape of the rod of equal deformations Δg , but differentiated by the parameter y_0 . For model, A we have the following lines:

- lines 1 – deflection $\Delta g = 3$ mm ($P_1 = 1.73$ cN for $y_0 = 2$ mm, $P_1 = 1.65$ cN for $y_0 = 0$ mm, $P_1 = 1.57$ cN for $y_0 = -2$ mm)
- lines 2 – deflection $\Delta g = 5$ mm ($P_1 = 3.49$ cN for $y_0 = 2$ mm, $P_1 = 3.35$ cN for $y_0 = 0$ mm, $P_1 = 3.20$ cN for $y_0 = -2$ mm).

For mode B, we have:

- lines 1 – deflection $\Delta g = 3$ mm ($P_1 = 3.073$ cN for $y_0 = 2$ mm, $P_1 = 3.08$ cN for $y_0 = 0$ mm, $P_1 = 3.07$ cN for $y_0 = -2$ mm)
- lines 2 – deflection $\Delta g = 5$ mm ($P_1 = 6.34$ cN for $y_0 = 2$ mm, $P_1 = 6.35$ cN for $y_0 = 0$ mm, $P_1 = 6.34$ cN for $y_0 = -2$ mm).

The differences in the bending forces that cause the same deflections result from the different geometries of the rods (parameter y_0). The rods are differentiated by shape (various functions describe the shape of these curves), and at the same time they have different curvature radii of these curves; the consequence of this is that different forces cause the same deformation. From the mathematical analysis results, it can be seen that the rod compressed according to model B is practically insensitive to the changes of parameter y_0 . Within the range that we tested, the parameter y_0 does not influence the value of the compressing force P_1 .

The third simulation concerns the influence of the monofilament's shape on the value of the compressing force. This is a problem of different buckling forms occurring, resulting in equal deflections of the same rod (and with the same geometry of fastening its ends), causing different values of force P_1 , and oppositely the same value of force P_1 may cause different deformations. The first case (equal values of deflection and different values of force P_1) is shown in Figure 5.

For a rod compressed according to model A, a deflection of $\Delta g = 5$ mm is caused by the forces P_1 of 3.48 cN, 3.62 cN, 10.39 cN, and 10.62 cN, whereas for a rod

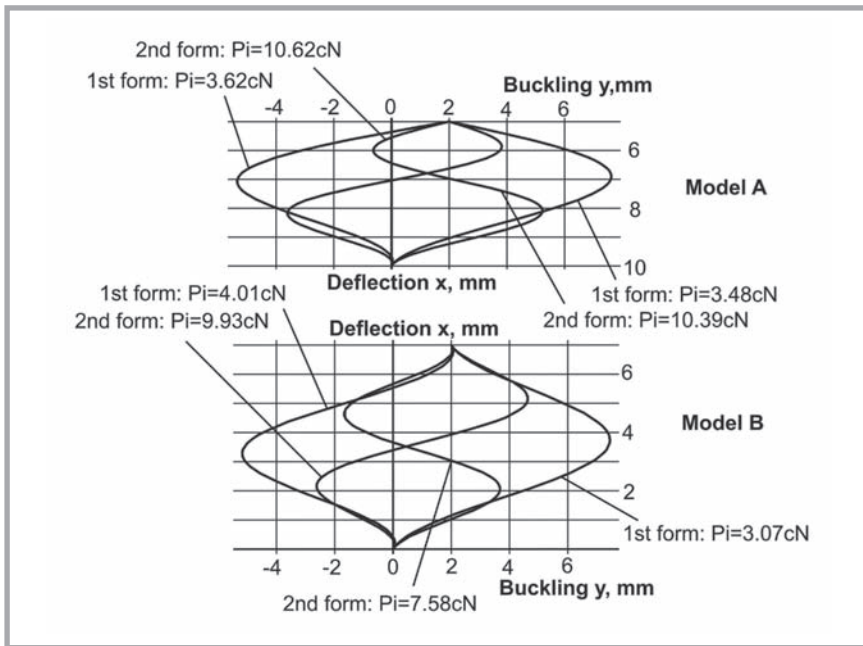


Figure 5. Different forms of the rod deflection caused by the action of different forces P_1 .

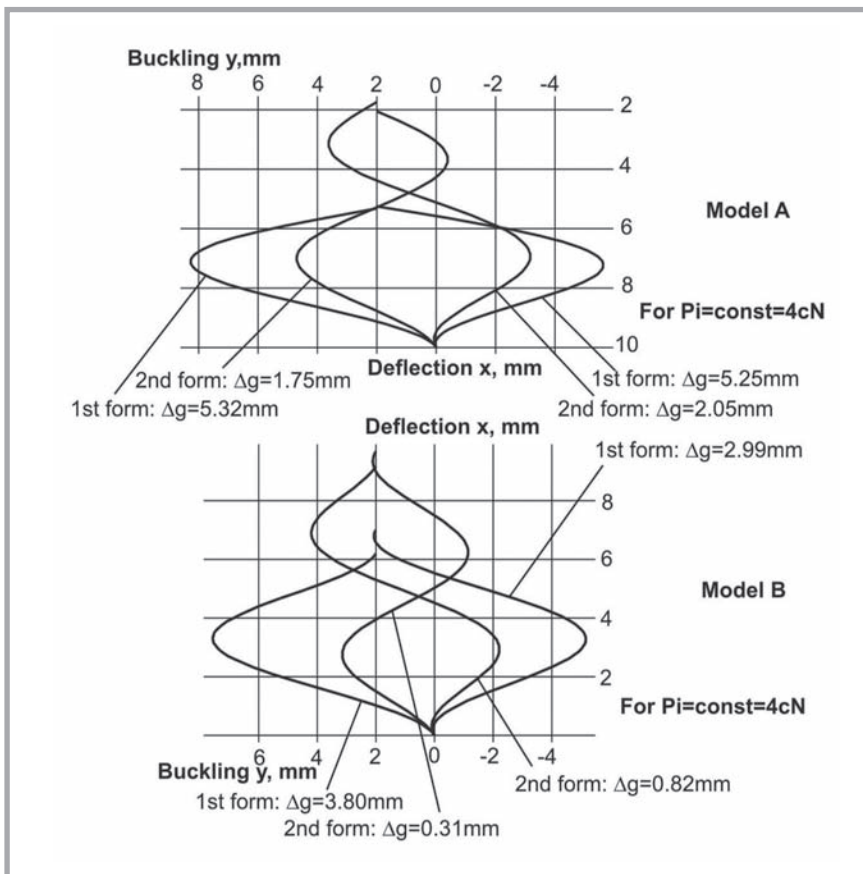


Figure 6. Different shapes of rod deflection caused by the impact of the same force.

compressed according to model B, a deflection of $\Delta g = 3$ mm is caused by P_1 of 3.07 cN, 4.01 cN, 9.93 cN, and 7.58 cN.

The second case (equal values of force P_1 causing different deflections Δg of the rod) is presented in **Figure 6**.

For the rod bent according to model A, the force $P_1 = 4$ cN causes deflections Δg of 1.75 mm, 2.05 mm, 5.25 mm, and 5.32 mm, whereas for that bent according to model B, the same force causes deflections of 3.80 mm, 2.99 mm, 0.81 mm, and 0.31 mm. The occurrence

of this phenomenon, which was confirmed empirically, may be explained in the following way: the greater the curvatures of the rod are, the greater value of force P_1 causes the same deflection Δg . This is clearly directly visible from the geometry of the compressed rods, as well as from the mathematical analysis carried out.

Summary

1. Physical and mathematical models of the compressing process of an elastic, slender rod with an assumed shape, fastened by one- or two-side fixed joints, are presented in this paper. The presented models are considered for compressing a 3D distance knitted fabric. The mechanical characteristics of the compressed rods were analysed and the rod's shapes discussed considering the aspect of the connector's tensions and the deformations of the knitted 3D fabric. The analysis of the phenomena of compressing the fabric included:

- the influence of the fastening geometry of a single monofilament on the value of the force compressing this monofilament.
- the influence of different forms of buckling of the compressed monofilament, which occur on the value of deflection Δg under the impact of the compressing force P_1 .

2. A computer simulation was carried out of the process of compressing a model concerned with the knitted fabric, which indicated that

- a change in the parameter y_0 (mutual displacement of the connectors' fastenings), in model B does not influence the value of force P_1 , whereas in model A, it causes changes within the range of 8%-10% of the P_1 value;
- in model A, for the second buckling form of the bent rod, the force P_1 is nearly 200% higher in comparison with the value for the first buckling form for the same deflection Δg . In model B, for the second form of buckling of the bent rod, the force P_1 is nearly 150% higher;
- in model A, for the second buckling form of the bent rod, the deflection Δg caused by the constant value of force P_1 is higher by nearly 175% in comparison with the value for the first buckling form. In model B, for the second buckling form, the bending of the rod is higher by 360%.

Conclusions

In the future parts of this research work, mathematical models will be presented of connectors considering mutual displacements of the outside layers of the knitted fabric. In parallel, we will conduct activity into designing and building an experimental model related to the three models of the 3D distance knitted fabric that we elaborated. This model will also be aimed to verify further mathematical models describing the displacement of the outer layers of the 3D distance knitted fabric mentioned in this paper. The next stage of our work will be the development of an elaboration model for knitted fabrics loaded non-uniformly and loaded by way of objects with a given shape.

The solutions presented herein should be considered as an introduction to further research work aimed at finding optimum calculation models for 3D distance knitted fabrics in order to determine the mechanical properties of these fabrics, but firstly at estimating their susceptibility to compression, as well as adaptation of the calculation mechanism created for solving real problems occurring while designing and applying 3D distance knitted fabrics.



References

1. Kopias K., „Technologia dzianin kolumniowych”, Ed. WNT, Warszawa 1986.
2. Żurek W., Kopias K., „Struktura płaskich wyrobów włókienniczych”, Ed. WNT, Warszawa 1983.
3. Niezgodziński M. E., Niezgodziński T., „Wytrzymałość materiałów”, Ed. PWN, Warszawa 2000.
4. Misiak J., „Stateczność konstrukcji prętowych”, Ed. PWN, Warszawa 1990.
5. Bodnar A., „Wytrzymałość materiałów”, Politechnika Krakowska, Kraków 2004.
6. Misiak J., „Obliczenia konstrukcji prętowych”, Ed. PWN, Warszawa 1993.
7. Biegus A., „Nośność graniczna stalowych konstrukcji prętowych”, Ed. PWN, Warszawa-Wrocław 1997.
8. Supel B., Mikołajczyk Z., „Model procesu ściskania łącznika zamocowanego przegubowo dzianiny dystansowej 3D”, *Fibres and Textiles in Eastern Europe*, Vol. 16, No. 6 (71), pp. 40-44, 2008.
9. Mosurski R., „Mathematica”, Wydawnictwa Naukowo-Dydaktyczne, Kraków 2001.

Received 22.08.2007 Reviewed 30.10.2007



Institute of Biopolymers and Chemical Fibres Instytut Biopolimerów i Włókien Chemicznych IBWCh

Director of the Institute: Danuta Ciechańska Ph.D., Eng.

The research subject of IBWCh is conducting scientific and development research of techniques and technologies of manufacturing, processing, and application, into in the following fields:

- biopolymers,
- chemical fibres and other polymer materials and related products,
- pulp and paper industry and related branches

R&D activity includes the following positions, among others:

- biopolymers,
- functional, thermoplastic polymers,
- biodegradable polymers and products from recovered wastes,
- biomaterials for medicine, agriculture, and technique,
- nano-technologies, e.g. nano-fibres, and fibres with nano-additives,
- processing of fibres, films, micro-, and nano- fibrous forms, and nonwovens,
- paper techniques, new raw material sources for manufacturing paper pulps,
- environmental protection,

The Institute is active in implementing its works in the textile industry, medicine, agriculture, as well as in the cellulose, and paper industries.

The Institute is equipped with unique technological equipment, as the technological line for fibre (e.g. cellulose, chitosan, starch, and alginate) spinning by the wet method.

The Institute organises educational courses and workshops in fields related to its activity.

The Institute's offer of specific services is wide and differentiated, and includes:

- physical, chemical and biochemical investigations of biopolymers and synthetic polymers,
- physical, including mechanical investigation of fibres, threads, textiles, and medical products,
- tests of antibacterial and antifungal activity of fibres and textiles,
- investigation in biodegradation,
- investigation of morphological structures by SEM and ESEM
- investigation and quality estimation of fibrous pulps, card boards, and paper products, including paper dedicated to contact with food, UE 94/62/EC tests, among others.
- Certification of paper products.

The Institute is active in international cooperation with a number of corporation, associations, universities, research & development institutes and centres, and companies.

The Institute is publisher of the scientific journal 'Fibres and Textiles in Eastern Europe'.

Instytut Biopolimerów i Włókien Chemicznych (IBWCh)

Institute of Biopolymers and Chemical Fibres

ul. Skłodowskiej-Curie 19/27; 90-570 Łódź, Poland

Phone: (48-42) 638-03-02, Fax: (48-42) 637-65-01

E-mail: ibwch@ibwch.lodz.pl <http://www.ibwch.lodz.pl>